Patient Respiratory-Triggered Quantitative T_2 Mapping in the Pancreas

Naïk Vietti Violi, MD,[1*] Tom Hilbert, PhD,[1,2,3] Jessica A.M. Bastiaansen, PhD,[1] Jean-Francois Knebel, PhD,[4,5] Jean-Baptiste Ledoux, BS,[1,4] Alto Stemmer, MSc,[6] Reto Meuli, MD,[1] Tobias Kober, PhD,[1,2,3] and Sabine Schmidt, MD[1]

Background: Long acquisition times and motion sensitivity limit T_2 mapping in the abdomen. Accelerated mapping at 3 T may allow for quantitative assessment of diffuse pancreatic disease in patients during free-breathing.
Purpose: To test the feasibility of respiratory-triggered quantitative T_2 analysis in the pancreas and correlate T_2-values with age, body mass index, pancreatic location, main pancreatic duct dilatation, and underlying pathology.
Study Type: Retrospective single-center pilot study.
Population: Eighty-eight adults.
Field Strength/Sequence: Ten-fold accelerated multiecho-spin-echo 3 T MRI sequence to quantify T_2 at 3 T.
Assessment: Two radiologists independently delineated three regions of interest inside the pancreatic head, body, and tail for each acquisition. Means and standard deviations for T_2 values in these regions were determined. T_2-value variation with demographic data, intraparenchymal location, pancreatic duct dilation, and underlying pancreatic disease was assessed.
Statistical Tests: Interreader reliability was determined by calculating the interclass coefficient (ICCs). T_2 values were compared for different pancreatic locations by analysis of variance (ANOVA). Interpatient associations between T_2 values and demographical, clinical, and radiological data were calculated (ANOVA).
Results: The accelerated T_2 mapping sequence was successfully performed in all participants (mean acquisition time, 2:48 ± 0:43 min). Low T_2 value variability was observed across all patients (intersubject) (head: 60.2 ± 8.3 msec, body: 63.9 ± 11.5 msec, tail: 66.8 ± 16.4 msec). Interreader agreement was good (ICC, 0.82, 95% confidence interval: 0.77–0.86). T_2-values differed significantly depending on age ($P < 0.001$), location ($P < 0.001$), main pancreatic duct dilatation ($P < 0.001$), and diffuse pancreatic disease ($P < 0.03$).
Data Conclusion: The feasibility of accelerated T_2 mapping at 3 T in moving abdominal organs was demonstrated in the pancreas, since T_2 values were stable and reproducible. In the pancreatic parenchyma, T_2-values were significantly dependent on demographic and clinical parameters.
Level of Evidence: 4
Technical Efficacy: Stage 1

J. MAGN. RESON. IMAGING 2019;50:410–416.

WHILE T_1- AND T_2-WEIGHTED IMAGING are the mainstay of most clinical magnetic resonance imaging (MRI) protocols, high-resolution parametric T_2 maps can be clinically relevant for measuring tissue properties.[1] Unlike conventional MR sequences, which evaluate morphological alterations, T_2 mapping (or T_2 relaxometry) enables quantification of the transverse relaxation time of the underlying tissues.[2] This evaluation is assumed to be more sensitive and reproducible than the visual assessment of T_2-weighted MR images for identifying minor contrast changes (eg, tissue edema).[3] For this reason, it is applied for quantifying well-defined pathologies (eg, cardiac iron overload or cartilage degeneration).[4,5]

View this article online at wileyonlinelibrary.com. DOI: 10.1002/jmri.26612

Received Sep 18, 2018, Accepted for publication Nov 26, 2018.

*Address reprint requests to: N.V.V., Rue du Bugnon 46, 1011 Lausanne, Switzerland. E-mail: naik.vietti-violi@chuv.ch

From the [1]Department of Radiology, University hospital (CHUV) and University of Lausanne (UNIL), Lausanne, Switzerland; [2]Advanced Clinical Imaging Technology, Siemens Healthcare, Switzerland; [3]LTS5, École Polytechnique Fédérale de Lausanne, Lausanne, Switzerland; [4]Center for Biomedical Imaging (CIBM), Lausanne, Switzerland; [5]Laboratory for investigative neurophysiology (The LINE), Department of Radiology and Department of Clinical Neurosciences, University hospital center and University of Lausanne, Lausanne, Switzerland; and [6]Siemens Healthcare, Erlangen, Germany

Additional supporting information may be found in the online version of this article.

T_2 mapping has been introduced into clinical practice for various organs and tissues, including brain,[6–8] heart,[4,9] and cartilage.[5,10–12] In neuroradiology, a microstructural change, such as neuronal loss or demyelination, results in increased free water and thus longer T_2 relaxation times and greater signal intensity on T_2-weighted MRI images.[13] Furthermore, T_2 mapping is used to assess cartilage damage in musculoskeletal imaging[10–12] and to evaluate cardiac edema and fibrosis.[9]

T_2 mapping in the abdomen has proven more difficult because of movement of the abdominal organs with breathing. In addition, bowel peristalsis can result in motion artifacts. However, the technique has already been successfully applied in the liver for diffuse disease, such as iron overload[14] and cirrhosis.[2,15] Of note, in one of these reports analysis of the left liver lobe was avoided because of motion artifact.[2] Otherwise, motion as a limitation has not been addressed, mainly because of attention to analysis of diffuse parenchyma and not focal lesions.

Pancreatic T_2 mapping has been successfully performed in a few healthy volunteers at 1.5 and 3 T,[16–18] but the technique has yet to be investigated in a patient population. Furthermore, because motion artifacts are invariably associated with long acquisition times in quantitative imaging, T_2 mapping in abdominal organs has not been widely performed. However, recent work validated a novel quantitative MRI sequence for T_2 mapping in the brain, which drastically shortened acquisition time compared with previously used methods.[19] A similar strategy also might enable reproducible T_2 mapping in moving abdominal organs.

Although pancreatic T_1 mapping has already been successfully applied for assessing chronic pancreatitis,[20,21] T_2 mapping in the pancreas also is of clinical interest. In acute pancreatitis, inflammatory cell recruitment induces parenchymal changes, including edema that lengthens the T_2 relaxation time,[22] typically observed as increased T_2-weighted signal. Pancreatic T_2 mapping could enable quantification of T_2 changes caused by underlying edema and inflammation, offering a means of objective staging. However, before pathology can be assessed, reference values need to be established, as does an overview of how findings vary with different clinical parameters.

The primary goal of this pilot study therefore was to demonstrate the feasibility of rapid and respiratory-triggered pancreatic T_2 mapping to obtain reproducible T_2 values. The secondary goal was to investigate quantitative differences in T_2 values as they relate to age, body mass index (BMI), and sex. The third goal was to assess the correlation between pancreatic T_2 values, anatomical region (head, body, tail), pancreatic duct dilatation, and underlying pancreatic disease.

1. Materials and Methods

1.1 Study Design

This retrospective, single-center pilot study was approved by the Institutional Review Board. Informed written consent was waived. From September 2016 to January 2017, a prototype T_2-mapping MR sequence was included in our dedicated liver MRI protocol with the goal of improving the assessment of liver cirrhosis, particularly in case of iron overload.[2,14,15] We reviewed all patients who underwent liver MRI with T_2 mapping (n = 93) and were adults (age > 18 years). We excluded five of this group from the analysis. These were patients in whom the identification of the pancreas parenchyma on the MR images was impossible because of complete pancreatic fat involution (n = 1) or complete surgical removal (n = 1), and patients in whom the T_2 mapping MRI prototype sequence had a technical problem in the image reconstruction, failing to provide T_2 maps (n = 3). The study population thus consisted of 88 patients (46 women, 52%), with a mean age of 57 years (range: 24–93, standard deviation [SD]: 17.2) and mean BMI of 24 kg/m^2 (range: 17–39, SD: 4.1).

1.2 MR Data Acquisition and Reconstruction

Patients underwent a conventional liver MRI examination during which the T_2 mapping prototype sequence was acquired. To prevent stochastic peristaltic movement, the patients were asked to fast for 6 hours before the MRI exam, and an intravenous injection of 10 mg scopolamine (Buscopan) was administered prior to the exam. All patients were scanned in a supine position at 3 T (Magnetom Skyra [n = 4], Skyra-Fit [n = 75], and PrismaFit [n = 9], Siemens Healthcare, Erlangen, Germany) using an 18-channel body array coil and a 32-channel spine coil. A multiecho spin-echo (MESE)[23] prototype sequence was used to acquire a 10-fold undersampled k-space using prospective acquisition correction (PACE)[24] with external triggering (15 slices, 0.8 × 0.8 × 5 mm resolution, ΔTE/TR/TA 10.6 msec/2.2 sec/2:39 min). According to the individual trigger efficiency of a patient, the MR technician chose either a phase scout or a 1D navigator at the liver dome to trigger the acquisition on end-expiration, thus allowing free breathing for the patients. For the reconstruction of T_2 maps, a combination of generalized autocalibrating partially parallel acquisition (GRAPPA)[25] and model-based accelerated relaxometry by iterative nonlinear inversion (MARTINI),[26] termed GRAPPATINI,[19] was employed. Furthermore, synthetic T_2-weighted images with different simulated echo times (TE = 40/100/150 msec) were generated by applying the forward signal model onto the quantitative maps.

1.3 Data Collection and Analysis

Two radiologists (N.V.V. and S.S.) with 5 and 15 years of experience in abdominal MRIs, respectively, reviewed the T_2 mapping sequence in all study patients. Each of the two readers separately reviewed the images on a picture archiving and communication system workstation (PACS; Carestream Vue, v. 11.4; Carestream Health, Rochester, NY). Patient information was masked to both radiologists during image analysis. Each radiologist determined the T_2 values (mean and SD) by manually drawing one region of interest (ROI) in each head, body, and tail of the pancreatic parenchyma (Fig. 1). The readers were instructed to draw the largest possible ROI in each area, while avoiding the pancreatic duct, vessels, focal lesions, and zones showing clear partial volume effects. They repeated the same analysis 3 weeks later to reduce recall bias. Furthermore, both radiologists performed a qualitative analysis of the pancreatic parenchyma in each case by reporting any pancreatic duct dilatation, defined by a maximal diameter of >4 mm, and any sign

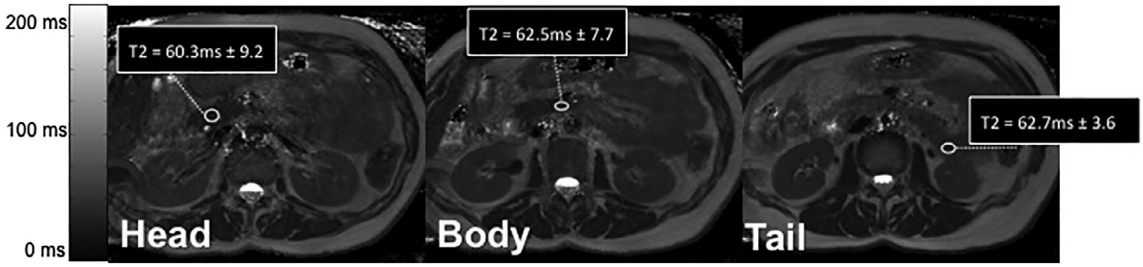

FIGURE 1: An axial T_2 map depicting the pancreas in one study patient. Each radiologist determined pancreas T_2 values by manually drawing regions of interest in the head, body, and tail of the pancreatic parenchyma, giving the mean T_2 value in each region of interest, including corresponding standard variation.

of diffuse pancreatic disease (acute or chronic pancreatitis, pancreatic fat infiltration). The two readers discussed any discordances until they reached a consensus.

One of the readers (N.V.V.) then reviewed electronic patient charts to collect demographic and clinical data (sex, age, BMI, and any possible diffuse/focal pancreatic disease). Finally, the acquisition time of the T_2 mapping sequence was extracted from the DICOM headers.

1.4 Statistical Analysis

Statistical analysis was performed with the commercially available software R (R Core Team (2013). R: A language and environment for statistical computing. R Foundation for Statistical Computing, Vienna, Austria. http://www.R-project.org/). The T_2 values separately determined by the two radiologists were compared using an adjusted interclass correlation coefficient (ICC) to assess intra- and interobserver reproducibility. According to Koo and Li, reliability was classified as poor (ICC < 0.5), moderate (ICC between 0.5 and 0.75), good (ICC between 0.75 and 0.9), or excellent (ICC > 0.90).[27]

Furthermore, the data from the two observers were averaged for the subsequent analyses. The mean T_2 value was compared in the same patient for the three pancreatic anatomical regions (head, body, and tail) and across all study patients. Finally, T_2 values were correlated in each patient with the corresponding demographic, clinical, and radiological data.

Categorical variables were compared using the chi-square test, and continuous variables with the Student's *t*-test, or analysis of variance (ANOVA) or Pearson correlation. Statistical differences were considered significant at $P < 0.05$.

2. Results

2.1 MR Data Acquisition and Reconstruction

In all 88 patients, the pancreatic parenchyma was clearly visible in both the T_2 maps and the simulated T_2-weighted images (Fig. 2). The mean acquisition time was 2 minutes, 50 seconds (range 2 min, 10 sec to 6 min, SD: 1 min 7 sec). The acquisition times depended mainly on patient breathing rhythm and trigger efficiency.

2.2 Data Collection and Analysis

Among the 88 study patients, 25 (28%) had main pancreatic duct dilation; all of chronic origin. Chronic pancreatic disease was identified in six patients (7%), either chronic pancreatitis ($n = 4$) or fatty involution ($n = 2$).

T_2 values were similar across all patients (intersubject), with low SD values (head: 60.3 ± 8.3 msec, body: 63.9 ± 11.5 msec, tail: 66.8 ± 16.4 msec). Inter- and intrareader reproducibility values are shown in Table 1. ICC was good between the two readers for the overall analyses (ICC = 0.820, 95% confidence interval [CI] = 0.774–0.857), as well as for each anatomical location (head: ICC = 0.794, 95% CI = 0.697–0.862; body: ICC = 0.806, 95% CI = 0.715–0.870; tail: ICC = 0.836, 95% CI = 0.757–0.891). Intrareader reproducibility was also mostly good, with only three exceptions showing moderate results (Table 1).

Figure 3 summarizes significant correlations between the T_2 values and patient characteristics. A significant correlation was found between T_2 values and age (r(238) = 0.347: $P < 0.001$). There also was a significant difference in T_2 values across the anatomical locations (head: 60.3 ± 8.3 msec; body: 63.9 ± 11.5 msec; tail: 66.8 ± 16.4 msec; F(2,158) = 12.566; $P < 0.001$) with significantly lower T_2 values in the pancreas head than in the body and tail. Mean T_2 values were significantly higher in patients with pancreatic duct dilatation compared with patients without main pancreatic duct dilatation (presence of dilatation: 76.6 ± 16.4, absence of dilatation: 59.3 ± 7.7 msec; t(238) = –10.943; $P < 0.001$). T_2 values were also significantly higher in patients with diffuse pancreatic disease compared with those with a healthy pancreas (presence of diffuse disease: 70.7 ± 9.2 msec, healthy pancreas: 63.2 ± 13 msec; t(238) = –2.187; $P < 0.03$). No significant correlations were found for sex (male: 64.7 ± 12.6 msec, female: 62.8 ± 13.2 msec, t(238) = 1.13; $P = 0.26$) and for BMI (r(238) = –0–063; $P = 0.335$).

3. Discussion

We demonstrated the feasibility of quantitative T_2 mapping in moving abdominal organs, in particular the pancreas, with a respiratory-triggered GRAPPATINI prototype. T_2 values in patients were stable and reproducible with mostly good reliability. Pancreatic T_2 values varied with anatomical location (highest in the tail of the pancreas) and we found a significant

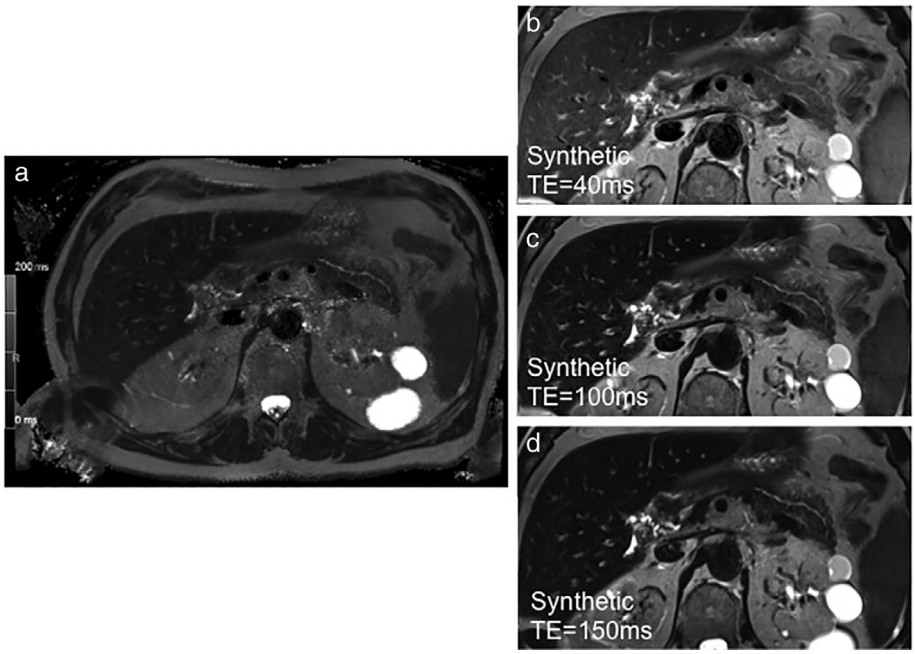

FIGURE 2: (A) Axial T_2 map depicting the pancreas in one study patient. Visual inspection enabled clear delineation of the pancreatic parenchyma (arrows), including the main duct (arrowhead). Multiple synthetic reconstructions of T_2-weighted images could be achieved at different TE times (B at 40 msec, C at 100 msec, and D at 150 msec).

TABLE 1. Inter- and intraobserver reproducibility (ICC (95% CI))

	Whole pancreas	Pancreatic head	Pancreatic body	Pancreatic tail
Interobserver reproducibility	0.820 (0.774–0.857)	0.794 (0.697–0.862)	0.806 (0.715–0.870)	0.836 (0.757–0.891)
Intraobserver reproducibility, 1st radiologist	0.742 (0.680–0.793)	0.542 (0.369–0.679)	0.736 (0.619–0.821)	0.880 (0.820–0.921)
Intraobserver reproducibility, 2nd radiologist	0.864 (0.829–0.893)	0.854 (0.782–0.903)	0.837 (0.758–0.891)	0.880 (0.820–0.921)

ICC: interclass correlation coefficient; CI: confidence interval.

correlation between T_2 values and age, pancreatic duct dilatation, and diffuse pancreatic disease.

De Bazelaire et al determined T_1- and T_2-values of various abdominal organs in six healthy volunteers, comparing results obtained at 1.5 T with those at 3 T.[17] Pancreatic T_2-values were 46 $\pm$ 6 msec at 1.5 T and 43 $\pm$ 7 msec at 3 T, both lower ranges than in the current study. Hoad et al analyzed T_2 values in various abdominal organs at 3 T in 10 healthy volunteers and also reported pancreatic values (42 $\pm$ 20 msec) lower than ours.[18] Both groups used T_2 prepared sequences with different readout techniques: HASTE for the former and balanced steady-state free-precession (bSSFP) for the latter. We chose the MESE approach because T_2 preparation may add further sensitivity to system imperfections, namely B_1 and B_0 inhomogeneity. Furthermore, a HASTE readout uses the entire echo train to sample the *k*-space, which will introduce T_2 blurring. On the other hand, bSSFP readouts are sampling-efficient but sensitive to B_0 field inhomogeneity, which leads to banding artifacts. Upadhyay et al recently reported results on T_2 mapping of the pancreas in 10 volunteers at 1.5 T.[16] The values presented here are in line with their results (57.8 msec to 63.14 msec). Of note, they used an imaging sequence similar to the MESE sequence used here, but with different sequence parameters (resolution, TR, ΔTE, echo-train length) and without acceleration. The reconstruction of the prototype sequence here does not account for stimulated echoes, leading to a slight T_2 overestimation, as discussed previously; this effect is typical for MESE sequences.[19] However, good to high reproducibility within and across participants has been demonstrated by Upadhyay et al as well as in the current study.

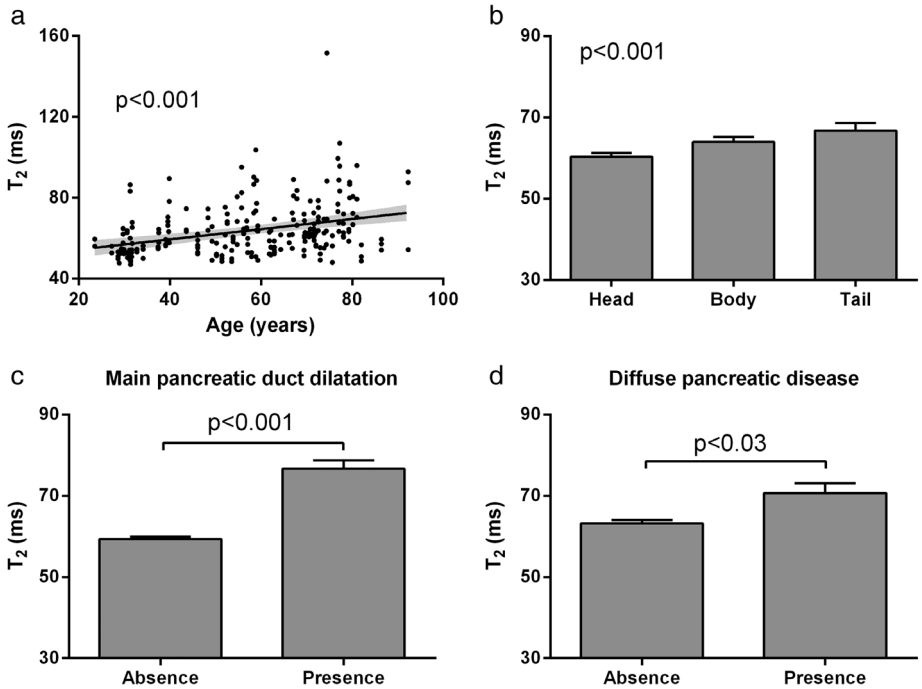

FIGURE 3: Histograms and charts of the statistically significant correlations between mean T_2 values and patient characteristics (age (A), pancreatic anatomical regions (B), presence of main pancreatic duct dilatation (C), and presence of diffuse pancreatic disease (D)).

The scan times in this study were shorter and provided much higher resolution images with whole pancreas coverage compared with Upadhyay et al (8 min vs. 2 min 50 sec). The sequence acquisition time depends mostly on the trigger efficiency and breathing rate of the patient. Trigger efficiency may be poor in noncooperative patients, prolonging the acquisition time. However, the mean acquisition time here was 2 min 50 sec, with a higher range of 6 min that was still lower than in the comparative study. The faster acquisition, enabled by GRAPPATINI with high (10-fold) acceleration, is also advantageous regarding motion artifacts because bulk motion is less likely to happen during shorter acquisition times.[28] Hence, GRAPPATINI may help in moving towards routine clinical applications of quantitative T_2 in the abdomen.

T_2 values differed with pancreatic anatomical location and were higher in the tail and lower in the head. Because no fat suppression was used, the correlation could have resulted from differences in fat infiltration among regions, with the most important region being the tail. However, this assumption seems unlikely; T_2 values were lower in the head (compared with body and tail) and fat replacement occurs predominantly in the head.[29] An erroneous inclusion of a slight amount of peripancreatic fat in the analysis also seems unlikely due to the low intra- and intraobserver variability in our values. Finally, this difference may be (partly) explained by the pancreatic craniocaudal anatomy, with the tail being thinner than the body and head and, thus, possibly inducing more partial volume effect.

We also found a significant correlation between T_2 values and age, in line with previous MRI studies showing that an association between fat infiltration of the pancreatic parenchyma and aging.[30] Because fat is characterized by high T_2-values, progressive fat infiltration with increasing age would also be expected to correlate positively with these T_2 values.

Multiple factors can explain the positive correlation between pancreatic duct dilatation and T_2 values. In this study, all main pancreatic duct dilatations were of chronic origin. Chronic main duct dilatation causes atrophy of the adjacent pancreatic parenchyma followed by increasing fat infiltration.[31] This setup would be expected to lead to higher T_2-values because no fat suppression was used. Kashiwagi et al reported a correlation between intraductal papillary mucinous neoplasm (a premalignant condition caused by papillary proliferation of pancreatic duct epithelium) and pancreatic fat content, suggesting that fat infiltration could be a risk for developing this neoplasm.[32]

Atrophy and consecutive fat infiltration may also explain the higher T_2 values with diffuse and chronic pancreatic disease.[31]

In the current study, we found no correlation between T_2 and sex, nor T_2 and BMI. Saisho et al also reported no association of T_2 with sex or age, obesity, or fat/parenchyma ratio (with only a slight difference in the pancreatic volume between males and females), in line with our results.[33] Two other studies that evaluated pancreatic fat content found no correlation between pancreatic fat infiltration and BMI

(or visceral fat area) as well.[32,34] This suggests that pancreatic fat infiltration is more caused by aging and atrophy than by obesity or sex.

This study has several limitations. First, as discussed above, we did not use fat suppression, so T_2 values may reflect underlying fat infiltration of the pancreas. However, current fat suppression techniques are imperfect and often result in heterogeneous suppression; for this reason, they can introduce bias depending on the spatial performance of the fat suppression. Second, some patients had diffuse liver disease, implying a selection bias towards this population. However, this study is the first to report pancreatic T_2 values in a patient population that are in agreement with previously reported values using the same sequence.[16] The third limitation is that the classification into healthy or pathologic pancreatic parenchyma was based on imaging features with no pathological reference standard. This classical limitation also occurs in patients with acute or chronic pancreatitis because the diagnosis is rarely based on pathology. We also made no comparison between different types of pancreatic diseases and patients with chronic pancreatitis or fat infiltration because of the low number of patients with pancreatic disease. A larger study population with pancreatic disease would be of great interest for quantitative MRI and could allow edema assessment using T_2 mapping. Because of the retrospective study design, we could not perform a scan and rescan analysis, but this analysis was done already in volunteers, with high reproducibility.[19]

As an alternative to T_2 mapping, the apparent transverse relaxation T_2* may be accessed instead using multiple gradient echo (GRE) breath-hold acquisitions. We chose the spin-echo T_2 relaxation over the GRE T_2* because local field inhomogeneity also affects T_2*. This local inhomogeneity can originate from tissue susceptibility, eg, from iron deposition. However, T_2* mapping is also sensitive to B_0 field inhomogeneity and leads to local overestimation if not correctly addressed. Although T_2* may be interesting for iron-related disease such as hemochromatosis, here we were investigating mostly inflammation, which we expect to affect the T_2 relaxation.

In conclusion, this study showed the feasibility of accelerated T_2 mapping at 3 T in moving abdominal organs, in particular the pancreas. T_2 values were reproducible within and between patients with moderate to good intra- and interobserver agreement. In the pancreatic parenchyma, T_2 values varied significantly depending on age, anatomical location, presence of pancreatic duct dilatation, and diffuse disease. The potential for quantitative analysis in the abdomen is of great interest and should be further investigated.

References

1. Shah B, Anderson SW, Scalera J, Jara H, Soto JA. Quantitative MR imaging: Physical principles and sequence design in abdominal imaging. Radiogr Rev Publ Radiol Soc N Am 2011;31:867–880.
2. Cassinotto C, Feldis M, Vergniol J, et al. MR relaxometry in chronic liver diseases: Comparison of T1 mapping, T2 mapping, and diffusion-weighted imaging for assessing cirrhosis diagnosis and severity. Eur J Radiol 2015;84:1459–1465.
3. Blystad I, Warntjes JBM, Smedby Ö, Lundberg P, Larsson E-M, Tisell A. Quantitative MRI for analysis of peritumoral edema in malignant gliomas. PLoS One 2017;12:e0177135.
4. Guo H, Au W-Y, Cheung JS, et al. Myocardial T2 quantitation in patients with iron overload at 3 Tesla. J Magn Reson Imaging 2009;30:394–400.
5. Apprich S, Mamisch TC, Welsch GH, et al. Quantitative T2 mapping of the patella at 3.0 T is sensitive to early cartilage degeneration, but also to loading of the knee. Eur J Radiol 2012;81:e438–e443.
6. Bauer S, Wagner M, Seiler A, et al. Quantitative T2′-mapping in acute ischemic stroke. Stroke 2014;45:3280–3286.
7. Seiler A, Lauer A, Deichmann R, et al. Complete restitution of the ischemic penumbra after successful thrombectomy?: A pilot study using quantitative MRI. Clin Neuroradiol 2018 [Epub ahead of print].
8. Sollmann N, Weidlich D, Cervantes B, et al. High isotropic resolution T2 mapping of the lumbosacral plexus with T2-prepared 3D turbo spin echo. Clin Neuroradiol 2018 [Epub ahead of print].
9. Spieker M, Katsianos E, Gastl M, et al. T2 mapping cardiovascular magnetic resonance identifies the presence of myocardial inflammation in patients with dilated cardiomyopathy as compared to endomyocardial biopsy. Eur Heart J Cardiovasc Imaging 2018;19:574–582.
10. Nguyen JC, Liu F, Blankenbaker DG, Woo KM, Kijowski R. Juvenile osteochondritis dissecans: Cartilage T2 mapping of stable medial femoral condyle lesions. Radiology 2018;171995.
11. Albano D, Chianca V, Cuocolo R, et al. T2-mapping of the sacroiliac joints at 1.5 Tesla: A feasibility and reproducibility study. Skeletal Radiol 2018 [Epub ahead of print].
12. Pachowsky ML, Kleyer A, Wagner L, et al. Quantitative T2 mapping shows increased degeneration in adjacent intervertebral discs following kyphoplasty. Cartilage 2018;1947603518758434.
13. Martin P, Bender B, Focke NK. Post-processing of structural MRI for individualized diagnostics. Quant Imaging Med Surg 2015;5:188–203.
14. Ruefer A, Bapst C, Benz R, et al. Role of liver magnetic resonance imaging in hyperferritinaemia and the diagnosis of iron overload. Swiss Med Wkly 2017;147:w14550.
15. Guimaraes AR, Siqueira L, Uppal R, et al. T2 relaxation time is related to liver fibrosis severity. Quant Imaging Med Surg 2016;6:103–114.
16. Upadhyay J, Dolgopolov S, Narang J, et al. Prospective assessment of variability and reproducibility of diffusion-weighted MRI and T2-mapping of the pancreas in healthy volunteers. J Med Imaging Case Rep 2017;01.
17. de Bazelaire CMJ, Duhamel GD, Rofsky NM, Alsop DC. MR imaging relaxation times of abdominal and pelvic tissues measured in vivo at 3.0 T: Preliminary results. Radiology 2004;230:652–659.
18. Hoad CL, Cox EF, Gowland PA. Quantification of T(2) in the abdomen at 3.0 T using a T(2)-prepared balanced turbo field echo sequence. Magn Reson Med 2010;63:356–364.
19. Hilbert T, Sumpf TJ, Weiland E, et al. Accelerated T2 mapping combining parallel MRI and model-based reconstruction: GRAPPATINI. J Magn Reson Imaging 2018 [Epub ahead of print].
20. Tirkes T, Lin C, Fogel EL, Sherman SS, Wang Q, Sandrasegaran K. T1 mapping for diagnosis of mild chronic pancreatitis. J Magn Reson Imaging JMRI 2017;45:1171–1176.
21. Wang M, Gao F, Wang X, et al. Magnetic resonance elastography and T1 mapping for early diagnosis and classification of chronic pancreatitis. J Magn Reson Imaging 2018 [Epub ahead of print].
22. Tang MY, Chen TW, Huang XH, et al. Acute pancreatitis with gradient echo T2*-weighted magnetic resonance imaging. Quant Imaging Med Surg 2016;6:157–167.
23. Carr HY, Purcell EM. Effects of diffusion on free precession in nuclear magnetic resonance experiments. Phys Rev 1954;94:630–638.

24. Zech CJ, Herrmann KA, Huber A, et al. High-resolution MR-imaging of the liver with T2-weighted sequences using integrated parallel imaging: Comparison of prospective motion correction and respiratory triggering. J Magn Reson Imaging 2004;20:443–450.

25. Griswold MA, Jakob PM, Heidemann RM, et al. Generalized autocalibrating partially parallel acquisitions (GRAPPA). Magn Reson Med 2002;47: 1202–1210.

26. Sumpf TJ, Uecker M, Boretius S, Frahm J. Model-based nonlinear inverse reconstruction for T2 mapping using highly undersampled spin-echo MRI. J Magn Reson Imaging 2011;34:420–428.

27. Koo TK, Li MY. A guideline of selecting and reporting intraclass correlation coefficients for reliability research. J Chiropr Med 2016;15: 155–163.

28. Zaitsev M, Maclaren J, Herbst M. Motion artifacts in MRI: A complex problem with many partial solutions. J Magn Reson Imaging 2015;42: 887–901.

29. Matsumoto S, Mori H, Miyake H, et al. Uneven fatty replacement of the pancreas: Evaluation with CT. Radiology 1995;194:453–458.

30. Sato T, Ito K, Tamada T, et al. Age-related changes in normal adult pancreas: MR imaging evaluation. Eur J Radiol 2012;81:2093–2098.

31. Balci NC, Bieneman BK, Bilgin M, Akduman IE, Fattahi R, Burton FR. Magnetic resonance imaging in pancreatitis. Top Magn Reson Imaging 2009;20:25.

32. Kashiwagi K, Seino T, Fukuhara S, et al. Pancreatic fat content detected by computed tomography and its significant relationship with intraductal papillary mucinous neoplasm. Pancreas 2018 [Epub ahead of print].

33. Saisho Y, Butler A, Meier J, et al. Pancreas volumes in humans from birth to age one hundred taking into account sex, obesity, and presence of type-2 diabetes. Clin Anat 2007;20:933–942.

34. Kim SY, Kim H, Cho JY, et al. Quantitative assessment of pancreatic fat by using unenhanced CT: Pathologic correlation and clinical implications. Radiology 2014;271:104–112.